Reactivities of Representative Cyclopentadienyl η^4-*trans*-Diene Nitrosyl Complexes of Molybdenum toward Acetone[1,2]

Nancy J. Christensen, Peter Legzdins,* James Trotter,* and Vivien C. Yee

Department of Chemistry, The University of British Columbia, Vancouver, British Columbia, Canada V6T 1Z1

Received March 27, 1991

When CpMo(NO)(η^4-*trans*-butadiene) (Cp = η^5-C_5H_5) is treated with acetone, a ligand-coupling reaction occurs to form two complexes having the composition CpMo(NO)(η^4-$CH_2CHCHCH_2CMe_2O$), one in which the allyl portion of the coupled ligand is endo (**1A**) and one in which the allyl is exo (**1B**) with respect to the Cp ligand. Complete structural assignment of **1A** and **1B** has been effected by using NMR spectroscopic methods. Similar treatment of Cp*Mo(NO)(η^4-*trans*-butadiene) (Cp* = η^5-C_5Me_5) affords a single organometallic product, **2**, which is the Cp* analogue of **1A**. The coupling reaction between CpMo(NO)(η^4-*trans*-2,5-dimethyl-2,4-hexadiene) and acetone is fairly rapid, the initial products being the *endo*-allyl (**3A**) and *exo*-allyl (**3B**) complexes. The endo isomer, however, converts quickly and irreversibly to the *exo*-allyl isomer. If the latter reaction is left for 15 h at ambient conditions, then **3B** and [CpMo(NO)]$_3$(μ_2-η^2-η^1-O-CMe_2)$_3$, which is isolable as a THF solvate (**4**), are the only organometallic species present in the final reaction mixture. All new complexes isolated during this work have been fully characterized by conventional methods, and crystal structure analyses have been performed on **2**, **3B**, and **4**. Crystals of Cp*Mo(NO)(η^4-*endo*-$CH_2CHCHCH_2CMe_2O$) (**2**) are orthorhombic, $P2_12_12_1$, with a = 9.2465 (15) Å, b = 13.496 (2) Å, c = 14.290 (3) Å, and Z = 4; the structure was solved by conventional heavy-atom methods and was refined by full-matrix least-squares procedures to R = 0.030 and R_w = 0.034 for 1454 absorption-corrected reflections with $I \geq 3\sigma(I)$. Crystals of Cp(NO)Mo[η^4-$C(Me)_2CHCHC(Me)_2C(Me)_2O$] (**3B**) are triclinic $P\bar{1}$, with a = 9.381 (4) Å, b = 14.085 (6) Å, c = 14.563 (7) Å, α = 117.36 (3)°, β = 100.91 (4)°, γ = 96.37 (4)°, and Z = 4; R = 0.073 and R_w = 0.077 for 2577 reflections. Crystals of [CpMo(NO)]$_3$(μ_2-η^2-η^1-$OCMe_2$)$_3$·THF (**4**) are monoclinic, $P2_1/c$, with a = 14.726 (3) Å, b = 11.097 (4) Å, c = 19.369 (2) Å, β = 98.479 (11)°, and Z = 4; R = 0.040 and R_w = 0.066 for 3963 reflections. Complexes **2** and **3B** are monomeric and possess four-legged piano-stool molecular structures in the solid state. The allyl portions of the coupled ligands in these compounds are bonded somewhat asymmetrically (particularly in **2**) to the molybdenum centers, being oriented endo with respect to the Cp ligand in **2** and exo in **3B**. In contrast, the structure of **4** consists of three four-legged piano stool monomeric units connected by Mo–acetone–Mo linkages, the angles around the O-bound carbon of the bridging acetone group being quite distorted. The trimer **4** persists in the presence of excess acetone, but it can be broken with 1,3-(diphenylphosphino)propane (dppp) to form CpMo(NO)(dppp).

Introduction

We have previously established that the 14-electron Cp'Mo(NO) fragments [Cp' = Cp (η^5-C_5H_5) or Cp* (η^5-C_5Me_5)] readily bind acyclic, conjugated dienes.[3-5] The most interesting feature of the resulting 18-electron Cp'Mo(NO)(η^4-diene) complexes is that their thermodynamically most stable forms contain unusual types of metal–*trans*-diene linkages that apparently are manifestations of the frontier-orbital properties of the Cp'Mo(NO) fragments.[4] It is well-known that coordination of a diene to a metal center in any fashion alters the electronic structure of the diene group and thus changes its reactivity toward electrophiles and nucleophiles from that exhibited by the diene in the free state.[6] The availability of the Cp'Mo(NO)(η^4-*trans*-diene) complexes thus permits a detailed investigation of how the reactivity patterns of the diene ligands have been altered by virture of their mode of attachment to the molybdenum centers. This paper reports the results of such detailed reactivity studies. Specifically, the chemical transformations that occur when representative Cp'Mo(NO)(η^4-*trans*-diene) complexes are treated with acetone are described. We have previously reported the chemistry that occurs when these organometallic reactants are exposed to simple Lewis bases,[5] acetylenes,[1] and protonic acids.[1]

Experimental Section

All reactions and subsequent manipulations involving organometallic reagents were performed under anaerobic and anhydrous conditions using an atmosphere of dinitrogen. Conventional Schlenk techniques or a Vacuum Atmospheres Corp. Dri-Lab Model HE-43-2 drybox were employed for the manipulation of air- and moisture-sensitive compounds.[7,8] All reagents were purchased from commercial suppliers or were prepared according to their published procedures. Reagent purity was ascertained by elemental analysis and ^{1}H NMR spectroscopy. Florisil (60–100 mesh) was used for the preparation of chromatography columns. Solvents were dried according to conventional procedures,[9] distilled and deaerated with dinitrogen just prior to use. Acetone (BDH OmniSolv) was simply deaerated prior to use.

Infrared spectra were recorded on a Nicolet 5DX FT-IR instrument that was internally calibrated with a He/Ne laser. All ^{1}H and ^{13}C NMR spectra were obtained on a Varian Associates

(1) Organometallic Nitrosyl Chemistry. 48. For part 47, see: Christensen, N. J.; Legzdins, P.; Einstein, F. W. B.; Jones, R. H. *Organometallics*, in press.

(2) (a) Taken in part from: Christensen, N. J. Ph.D. Dissertation, The University of British Columbia, 1989. Yee, V. C. Ph.D. Dissertation, The University of British Columbia, 1990. (b) Presented in part at the 1989 International Chemical Congress of Pacific Basin Societies (PACIFICHEM '89), Honolulu, HI, Dec 1989, Abstract ORGN 314.

(3) Hunter, A. D.; Legzdins, P.; Nurse, C. R.; Einstein, F. W. B.; Willis, A. C. *J. Am. Chem. Soc.* **1985**, *107*, 1791.

(4) Hunter, A. D.; Legzdins, P.; Nurse, C. R.; Einstein, F. W. B.; Willis, A. C.; Bursten, B. E.; Gatter, M. G. *J. Am. Chem. Soc.* **1986**, *108*, 3843.

(5) Christensen, N. J.; Hunter, A. D.; Legzdins, P. *Organometallics* **1989**, *8*, 930.

(6) (a) Davies, S. G. *Organotransition Metal Chemistry: Applications to Organic Synthesis*; Pergamon Press: Oxford, England, 1982. (b) Collman, J. P.; Hegedus, L. S.; Norton, J. R.; Finke, R. G. *Principles and Applications of Organotransition Metal Chemistry*; University Science Books: Mill Valley, CA, 1987.

(7) Shriver, D. F.; Drezdzon, M. A. *The Manipulation of Air-Sensitive Compounds*, 2nd ed.; Wiley-Interscience: Toronto, 1986.

(8) Wayda, A. L.; Darensbourg, M. Y. *Experimental Organometallic Chemistry: A Practicum in Synthesis and Characterization*; ACS Symposium Series 357; American Chemical Society: Washington, DC, 1987.

(9) Perrin, D. D.; Armarego, W. L. F.; Perrin, D. R. *Purification of Laboratory Chemicals*, 2nd ed.; Pergamon Press: Oxford, England, 1980.

0276-7333/91/2310-4021$02.50/0

Table I. Elemental Analyses and Mass Spectral and Infrared Data for the Acetone-Coupled Products

complex no.	anal. found (calcd) C	H	N	infrared data ν_{NO}, cm^{-1} hexanes	Nujol mull	mass spectral data[a], m/z P^+ (T, °C)[b]
1A	47.61 (47.55)	5.73 (5.61)	4.62 (4.62)	1623	1587	305 (180)
1B	47.48 (47.55)	5.56 (5.61)	4.67 (4.62)	1603	1574	305 (180)
2	54.62 (54.72)	7.33 (7.24)	3.80 (3.75)	1616	1588	375 (170)
3A	53.70 (53.49)	7.00 (6.96)	3.77 (3.90)	1632	1630, 1603	303 (100)[c]
3B	53.23 (53.49)	6.88 (6.96)	3.85 (3.90)	1616	1614, 1578	303 (100)[c]

[a] Assignments for ^{98}Mo. [b] Probe temperature. [c] Highest mass peak observed, ($P^+ - Me_2CO$).

Table II. ^1H NMR Data for the Acetone-Coupled Products

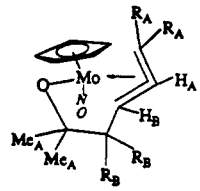

complex no.	chemical shifts δ, ppm Cp	Me_A	H_A	H_B	R_A	R_B
1A	5.22 (s)	1.60 (s)	5.62 (m)	4.75 (m)	2.08 (m)	1.88–2.20 (m)
		1.44 (s)			1.20 (m)	
1B	5.22 (s)	1.43 (s)	5.72 (m)	4.81 (m)	2.02 (m)	1.55–1.75 (m)
		0.99 (s)			1.50 (m)	
2	1.59 (s)	1.44 (s)	5.95 (m)	4.13 (m)	1.98 (m)	1.92 (m)
		1.41 (s)			0.96 (m)	1.69 (m)
3A	5.22 (s)	1.58 (s)	5.85 (d)[a]	4.80 (d)[b]	1.53 (s)[c]	1.04 (s)[c]
		1.43 (s)			1.28 (s)	0.78 (s)
3B	5.24 (s)	1.65 (s)	5.84 (d)[d]	5.16 (d)[e]	1.26 (s)[c]	1.07 (s)[c]
		0.96 (s)			0.86 (s)	1.04 (s)

[a] J_{HH} = 13.7 Hz. [b] J_{HH} = 13.7 Hz. [c] Assignments of R_A vs R_B signals are tentative. [d] J_{HH} = 7.0 Hz. [e] J_{HH} = 7.0 Hz.

XL-300 or a Bruker WH-400 spectrometer with reference to the residual ^1H or ^{13}C signal of the solvent employed (usually C_6D_6). All ^1H and ^{13}C chemical shifts are reported in parts per million (ppm) downfield from Me_4Si. Ms. M. Austria, Ms. L. Darge, and Dr. S. O. Chan assisted in the collection of some of the NMR spectra. Low-resolution mass spectra were recorded at 70 eV on an Atlas CH4B or a Kratos MS50 spectrometer using the direct-insertion method by Dr. G. K. Eigendorf and the staff of the UBC Mass Spectrometry Laboratory; probe temperatures were between 100 and 150 °C. Elemental analyses were performed by Mr. P. Borda of this department.

NMR Experiments. Some nonroutine NMR experiments were conducted during this study. The specific experiments are described below.

(a) 2D Heterocorrelation NMR Experiments (2D-HETCOR). Varian's 2D-HETCOR pulse program was used in these experiments. The 90° ^{13}C pulse was 18 μs, the 90° ^1H pulse from the decoupler was 46 μs, the acquisition time was ca. 0.6 s, and presaturation was used. The number of incremental spectra was determined according to the concentration of the sample and spectral width used for collection of the FIDs. Zero-filling and a 2D Fourier transformation resulted in a spectrum with a resolution of ca. 6 and ca. 100 Hz in the proton and carbon dimensions, respectively. Depending on the specific requirements of the experiments, spectra with adequate signal-to-noise ratios were obtained in 6–16 h.

(b) 2D Correlation Spectroscopy (2D-COSY). These experiments were performed with Varian's pulse sequences on the XL-300 spectrometer. These homonuclear correlation spectra were collected by using a 90° ^1H pulse of 45 μs. A delay period of 1 s was used between acquisitions (0.32 s). A 2D Fourier transformation resulted in 2D spectra with adequate signal-to-noise ratios after 6–12 h of data collection, depending on the concentration of the individual sample.

Reaction of CpMo(NO)(η^4-*trans*-2,5-dimethyl-2,4-hexadiene) with Acetone. Method A. To a reaction flask containing CpMo(NO)(η^4-*trans*-2,5-dimethyl-2,4-hexadiene)[5] (0.30 g, 1.0 mmol) was added acetone (25 mL) by syringe. An IR spectrum of the yellow solution showed a band due to the nitrosyl ligand at 1591 cm^{-1}. The reaction mixture was stirred for ca. 1.5 h, whereupon the color gradually changed to orange, and the IR spectrum indicated that the ν_{NO} had shifted to 1608 cm^{-1}. The acetone was removed under reduced pressure to leave an oily brown residue. Extraction of this residue with hexanes (3 × 25 mL) produced a yellow solution (ν_{NO} 1632, 1616 cm^{-1}), which was filter-cannulated to another flask and concentrated in vacuo to ca. 20 mL. This solution was then chromatographed through a Florisil column (3 × 3 cm) made-up in hexanes with Et_2O as eluant. The yellow band that developed was eluted, the eluate was dried in vacuo, and the remaining residue was recrystallized from hexanes to obtain 0.20 g (56% yield) of CpMo(NO)[η^4-C-$(Me)_2CHCHC(Me)_2C(Me)_2O$] (**3B**) as a yellow, microcrystalline solid. A crystal suitable for X-ray crystallographic analysis was obtained by maintaining a concentrated hexanes solution of **3B** at −20 °C for 1 week. Physical and analytical data for this complex and the other analogues isolated during the study of the reactions of the *trans*-diene complexes with acetone are collected in Table I–IV.

After the first yellow band had been eluted from the Florisil column, THF/Et_2O (1:1) was used to develop a second yellow band, which was collected separately and was taken to dryness to obtain 0.10 g (28% yield) of a product (**3A**) that had the same elemental composition as the first product (**3B**) but quite different physical properties (see Tables I–IV). Attempts to obtain suitable crystals of **3A** for X-ray analysis were thwarted by its isomerization to **3B** in solutions.

Table III. ^{13}C NMR Data for the Acetone-Coupled Products

complex no.	chemical shifts δ, ppm Cp	C_1	C_2	C_3	C_4	C_A[a]	$C_{Me(a)}$[b]	R_A/R_B
1A	102.6 (d, p)	41.4 (t)	131.1 (d)	104.7 (d)	48.9 (t)	107.8 (s)	34.1 (q)	
							29.7 (q)	
1B	101.8 (d, p)	42.2 (t)	117.0 (d)	113.0 (d)	46.9 (t)	105.0 (s)	33.8 (q)	
							29.4 (q)	
2[c]	103.1 (s)	47.7 (d)	118.8 (d)	117.0 (d)	44.1 (t)	111.5 (s)	35.6 (q)	
							33.7 (q)	
3B	104.6 (d, p)	71.8 (s)	129.3 (d)	103.7 (d)	46.2 (s)	106.2 (s)	31.0 (q)	30.4 (q)
								24.6 (q)
								24.4 (q)
								20.8 (q)

[a] Quaternary carbon of acetone fragment. [b] Methyl carbons of acetone fragment. [c] This is Cp* = η^5-C_5Me_5. The methyl carbons resonate at 10.1 ppm.

Table IV. ^{13}C NMR Coupling Constants for the Acetone-Coupled Complexes

complex no.	coupling constants, Hz						
	Cp	C_1	C_2	C_3	C_4	$C_{Me(a)}$	R_A/R_B
1A	177.0[a]	155.2	156.0	156.0	129.0	124.0 125.5	
1B	177.0[a]	153.7	162.0	150.0	127.5 122.5	124.5	
2	b	150.5	160.0	150.0	122.5	124.2 125.0	
3B	175.6[a]		144.0	153.0		125.0	124.0 124.7 128.0 123.3

[a] $^2J_{CH} \simeq {}^3J_{CH}$ observed for the Cp complexes are as follows: 1A, 7.5; 1B, 6.0; 3B, 6.7 Hz. [b] This is Cp* = η^5-C_5Me_5. The methyl carbons exhibit $^1J_{CH}$ = 126.7 Hz.

Method B. In a manner similar to that outlined in method A, an acetone solution (25 mL) of CpMo(NO)(η^4-*trans*-2,5-dimethyl-2,4-hexadiene) (0.30 g, 1.0 mmol) was stirred, but overnight. Similar workup to that outlined in method A allowed isolation of the first complex (**3B**) in 20% yield. Extraction of the hexanes-insoluble residue from the original reaction mixture with THF (3 × 15 mL) yielded a yellow solution (ν_{NO} 1593 cm^{-1}). Concentration of the THF solution and cooling at −20 °C for several weeks produced yellow crystals of $[CpMo(NO)]_3(\mu_2$-η^2-η^1-$OCMe_2)_3$·THF (**4**) in 60% yield. A crystal suitable for single-crystal X-ray crystallographic analysis was selected from this material.

Anal. Calcd for $C_{28}H_{41}N_3O_7Mo_3$: C, 41.05; H, 5.00; N, 5.13. Found: C, 40.75; H, 4.89; N, 5.11. IR (Nujol mull): ν_{NO} 1587, 1576 cm^{-1}. IR (THF): ν_{NO} 1593 cm^{-1}. ^1H NMR (CD_3NO_2): δ 5.99 (s, 5 H, C_5H_5), 5.88 (s, 5 H, C_5H_5), 5.63 (s, 5 H, C_5H_5), 3.65, (m, 8 H, CH_2 × 4), 2.04 (s, 3 H, CH_3 × 2), 1.95 (s, 3 H, CH_3), 1.86 (s, 3 H, CH_3), 1.80 (m, 8 H, CH_2 × 4), 1.59 (s, 3 H, CH_3). ^{13}C NMR (CD_3NO_2): δ 104.93 (dp, $^1J_{CH}$ = 176 Hz, $^2J_{CH}$ = 7 Hz, C_5H_5), 104.71 (dp, $^1J_{CH}$ = 176 Hz, $^2J_{CH}$ = 6 Hz, C_5H_5), 104.16 (dp, $^1J_{CH}$ = 176 Hz, $^2J_{CH}$ = 7 Hz, C_5H_5), 96.70 (s, Me_2C–O), 94.04 (s, Me_2C–O), 92.27 (s, Me_2C–O), 68.66 (t, $^1J_{CH}$ = 140 Hz, CH_2), 31.13, 34.64, 33.74, 33.55, 32.84 (overlapping multiplets due to 6 × CH_3), 26.59 (t, $^1J_{CH}$ = 122 Hz, CH_2). Low-resolution mass spectrum (probe temperature, 150 °C): m/z 543, $[P - CpMoNO(Me_2CO)]^+$.

Reactions of Cp′Mo(NO)(η^4-*trans*-butadiene) Complexes with Acetone. Treatment of Cp′Mo(NO)(η^4-*trans*-butadiene) (Cp′ = Cp or Cp*) with acetone followed by the workup outlined in method A above led to the isolation and characterization of the new complexes CpMo(NO)(η^4-*endo*-$CH_2CHCHCH_2CMe_2O$) (**1A**), CpMo(NO)(η^4-*exo*-$CH_2CHCHCH_2CMe_2O$) (**1B**), and Cp*Mo(NO)(η^4-*endo*-$CH_2CHCHCH_2CMe_2O$) (**2**). Single crystals of **2** suitable for an X-ray crystallographic analysis were grown by maintaining a saturated hexanes solution of the complex at −20 °C for 1 week. Physical and analytical data for these complexes are included in Tables I–IV. In none of these cases was there any evidence for formation of any compounds analogous to the trimer **4** or any other nitrosyl-containing complexes.

Reaction of Complex 3B with Acetone. A solution of complex **3B** (0.15 g, 0.4 mmol) in acetone (25 mL) and THF (10 mL) was stirred at room temperature for 3 days. An IR spectrum of the final mixture showed that the ν_{NO} of the starting complex at 1595 cm^{-1} was no longer present and that one at 1587 cm^{-1} had developed. In addition, the color of the solution had changed from yellow to dark yellow. The acetone and THF were removed under reduced pressure, and the resulting brown residue was extracted with THF (3 × 10 mL). The THF extracts were filter-cannulated to another flask and dried to obtain 0.3 g of complex **4**.

Reaction of Complex 3B with 1,3-(Diphenylphosphino)propane (dppp). A solution of **3B** in THF (0.15 g, 0.4 mmol, ν_{NO} 1593 cm^{-1}) was treated with 1,3-(diphenylphosphino)propane (ca. 1 g, excess), and the mixture was stirred for 1 week until the only ν_{NO} evident in the IR spectrum of the solution was at 1561 cm^{-1}. Solvent was removed from the final mixture in vacuo, and the resulting orange powder was washed with hexanes (1 × 15 mL) and then Et_2O (2 × 10 mL). The orange solid was then dissolved in CH_2Cl_2 (20 mL) to yield an orange solution, which was concentrated to ca. 10 mL to induce crystallization and was then maintained at −5 °C for several days. From this cooled mixture was isolated by filtration (0.20 g, 0.3 mmol, 83% yield) of CpMo(NO)(dppp).

Anal. Calcd for $C_{32}H_{31}NOP_2Mo$: C, 63.71; H, 5.14; N, 2.32. Found: C, 63.43; H, 5.25; N, 2.41. ^1H NMR ($CDCl_3$): δ 5.10 (s, 5 H, C_5H_5), 6.9–7.8 (m, 20 H, $[P(C_6H_5)_2]_2$), 2.3–2.8 (m, 6 H, CH_2 × 3). IR (CH_2Cl_2): ν_{NO} 1549 cm^{-1}. IR (Et_2O): ν_{NO} 1584 cm^{-1}.

X-ray Crystallographic Analyses of Complexes 2, 3B, and 4. The X-ray structure determinations of the three nitrosyl complexes were performed in a similar manner. A suitable X-ray-quality crystal of each complex was obtained as described in the preceding paragraphs. Each crystal was mounted in a thin-walled glass capillary under N_2 and transferred to an Enraf-Nonius CAD4-F (in the case of **2** and **3B**) or a Rigaku AFC6S (for **4**) diffractometer equipped with graphite-monochromated MoKα radiation ($\lambda_{K\alpha1}$ = 0.709 30, $\lambda_{K\alpha2}$ = 0.713 59 Å). Final unit-cell parameters for each complex were obtained by least-squares analysis of $2(\sin\theta)/\lambda$ values for 25 well-centered high-angle reflections, i.e. $12.2 \le \theta \le 17.0°$ for **2**, $10.0 \le \theta \le 12.5°$ for **3B**, and $15.0 \le \theta \le 17.2°$ for **4**. The intensities of three standard reflections were measured every 1 h of X-ray exposure time during the data collection of all three complexes. The intensities of the standard reflections of **2** showed no appreciable variations in intensity with time, but those of **3B** and **4** exhibited some decrease in intensity (i.e. 5.7–7.4% for **3B**, and mean isotropic decay of 8.7% for **4**), and the latter data were thus scaled for this deterioration in crystal quality. The data were corrected for Lorentz and polarization effects and for absorption by using the Gaussian integration method.[10-12] Pertinent crystallographic and experimental parameters for the three complexes are summarized in Table V.

Interpretation of the Patterson function yielded the coordinates of the heaviest atoms in each structure. The structures of the three compounds were solved by conventional electron density methods and were refined by full-matrix least-squares methods on F, minimizing the function $\sum w(|F_o| - k|F_c|)^2$, where w was calculated from $w = [\sigma^2(F)]^{-1}$. The variable k was used to scale the calculated to the observed structure factors. Hydrogen atoms were placed in idealized positions based on difference Fourier maps, with thermal parameters $B = 1.2B$ (bonded atom), and were not refined but were repositioned after each cycle. Final refinement for **2** was carried out with non-hydrogen atoms described by anisotropic thermal motion. The enantiomer (**2**), which best fit the observed diffraction pattern $[R_w(1)/R_w(2) = 1.0027]$ at a confidence level of ca. 98%, was accepted as the more correct model.[13] Final refinement for **3B** was carried out with non-hydrogen atoms being permitted anisotropic thermal motion; the largest peaks of final residual electron density (ca. 1.6 e Å^{-3}) were located about 1.1 Å away from the two molybdenum atoms. Final cycles of refinement for **4** were performed with anisotropic thermal motion for non-hydrogen atoms. The non-hydrogen atoms of the THF solvate molecule were refined with isotropic thermal parameters in disordered sites with half occupancies; no attempt was made to include the hydrogen atoms of the solvent molecule in the refinement model.

Complex neutral-atom scattering factors were taken from ref 15. Final positional and equivalent isotropic thermal parameters (U_{eq} = $^1/_3$ × trace diagonalized U) for the complexes are given in Tables VI–VIII. Selected bond lengths (Å) and bond angles (deg) for the compounds are listed in Table IX. Anisotropic thermal parameters, hydrogen parameters, full listings of mo-

(10) The computer programs used include locally written programs for data processing and locally modified versions of the following: ORFLS, full-matrix least squares, and ORFFE, function and errors, by W. R. Busing, K. O. Martin, and H. A. Levy; FORDAP, Patterson and Fourier syntheses, by A. Zalkin; ORTEPII, illustrations, by C. K. Johnson.

(11) Coppens, P.; Leiserowitz, L.; Rabinovich, D. *Acta Crystallogr.* **1965**, *18*, 1035.

(12) Busing, W. R.; Levy, H. A. *Acta Crystallogr.* **1967**, *22*, 457.

(13) The ratio $R_w(1)/R_w(2)$ was subjected to Hamilton's significance R-factor test,[14] i.e. $R_{1,1156,0.025} \simeq 1.0025$, where 1 is the degree of freedom, 1156 is the difference between the number of observations and the number of parameters, and 0.025 in the significance level.

(14) Hamilton, W. C. *Acta Crystallogr.* **1965**, *18*, 502.

(15) *International Tables for X-ray Crystallography*; Kynoch Press: Birmingham, England 1974; Vol. IV, Tables 2.2B and 2.3.1.

Table V. Crystallographic and Experimental Data[a] for the Complexes Cp*Mo(NO)(η^4-*endo*-$CH_2CHCHCH_2CMe_2O$) (2), CpMo(NO)[η^4-*exo*-$C(Me)_2CHCHC(Me)_2C(Me)_2O$] (3B), and [CpMo(NO)]$_3$($\mu_2$-$\eta^2$-$\eta^1$-$OC(Me_2)_3$•THF (4)

	2	3B	4
formula	$C_{17}H_{27}NO_2Mo$	$C_{16}H_{25}NO_2Mo$	$C_{28}H_{41}N_3O_7Mo_3$
fw	373.33	359.30	819.47
cryst syst	orthorhombic	triclinic	monoclinic
space group	$P2_12_12_1$	$P\bar{1}$	$P2_1/c$
a, Å	9.2465 (15)	9.381 (4)	14.726 (3)
b, Å	13.496 (2)	14.085 (6)	11.097 (4)
c, Å	14.290 (3)	14.563 (7)	19.369 (2)
α, deg	90	117.36 (3)	90
β, deg	90	100.91 (4)	98.479 (11)
γ, deg	90	96.37 (4)	90
V, Å^3	1738.2 (5)	1634.3 (14)	3131 (2)
Z	4	4	4
D_{calcd}, Mg m^{-3}	1.39	1.46	1.74
$F(000)$	776	744	1648
μ(Mo Kα), cm^{-1}	7.21	7.84	12.02
temp, K	293	293	293
cryst dimens, mm^3	0.14 × 0.50 × 0.35	0.20 × 0.24 × 0.38	0.10 × 0.20 × 0.33
λ(Mo Kα radiation) Å	0.71069	0.71069	0.71069
transm factors	0.90–0.91	0.84–0.88	0.96–1.00
scan type	coupled ω–2 θ	coupled ω–2 θ	coupled ω–2 θ
scan range, deg	0.80 + 0.35 tan θ	0.80 + 0.35 tan θ	1.63 + 0.35 tan θ
scan speed, deg min^{-1}	1.55–20.12	1.26–10.06	32.0 (up to 9 scans)
2θ limits, deg	$0 \le 2\theta \le 55$	$0 \le 2\theta \le 55$	$0 \le 2\theta \le 55$
no. of data collcd	$+h,+k,+l$	$\pm h,-k,\pm l$	$+h,+k,\pm l$
no. of unique reflns	2329	7477	7837
no. of reflns with $I \ge 3\sigma(I)$	1454	2577	3963
no. of variables	190	361	365
R_F[b]	0.030	0.073	0.040
R_{wF}[c]	0.034[d]	0.077[d]	0.066[d]
goodness of fit[e]	1.05	2.084	1.786
max Δ/σ (final cycle)	0.022	0.015	0.019
residual density, e Å^{-3}	0.33	1.59	0.74

[a] Enraf-Nonius CAD4-F diffractometer, Mo Kα radiation, graphite monochromator. [b] $R_F = \sum||F_o| - |F_c||/\sum|F_o|$. [c] $R_{wF} = [\sum w(|F_o| - |F_c|)^2/\sum F_o^2]^{1/2}$. [d] $w = [\sigma^2(F)]^{-1}$. [e] GOF = $[\sum w(|F_o| - |F_c|)^2/(\text{no. of degrees of freedom})]^{1/2}$.

Table VI. Final Positional (Fractional × 10^4, Mo × 10^5) and Equivalent Isotropic Thermal Parameters (10^3U, Å^2), for Cp*Mo(NO)(η^4-*endo*-$CH_2CHCHCH_2CMe_2O$) (2)

atom	x	y	z	U_{eq}
Mo	35640 (5)	69296 (4)	22877 (4)	41
O1	3441 (9)	4976 (4)	3235 (4)	105
O2	3074 (4)	7826 (3)	3384 (3)	51
N	3577 (7)	5794 (4)	2903 (3)	61
C1	1171 (6)	7131 (5)	1846 (5)	56
C2	1853 (7)	8042 (6)	1559 (4)	61
C3	2853 (8)	7805 (5)	860 (4)	55
C4	2786 (7)	6776 (5)	699 (4)	53
C5	1750 (7)	6367 (5)	1289 (5)	59
C6	−29 (8)	7046 (10)	2552 (5)	106
C7	1502 (12)	9034 (6)	1946 (6)	98
C8	3792 (12)	8538 (7)	329 (6)	91
C9	3552 (11)	6236 (6)	−95 (5)	91
C10	1265 (11)	5292 (5)	1269 (6)	88
C11	4055 (7)	8012 (6)	4127 (4)	63
C12	3398 (12)	8838 (6)	4728 (5)	87
C13	4259 (10)	7085 (6)	4717 (5)	84
C14	5489 (8)	8348 (6)	3679 (5)	78
C15	5642 (7)	7901 (5)	2727 (6)	68
C16	6028 (6)	6975 (7)	2528 (5)	75
C17	5708 (8)	6573 (6)	1631 (6)	74

lecular dimensions, and tables of calculated and observed structure factors for the three complexes are provided as supplementary material. Views of the solid-state molecular structures of Cp*Mo(NO)(η^4-*endo*-$CH_2CHCHCH_2CMe_2O$) (2), CpMo(NO)[η^4-$C(Me)_2CHCHC(Me)_2C(Me)_2O$] (3B), and [CpMo(NO)]$_3$($\mu_2$-$\eta^2$-$\eta^1$-$OCMe_2$)$_3$•THF (4) are displayed in Figures 1–3, respectively.

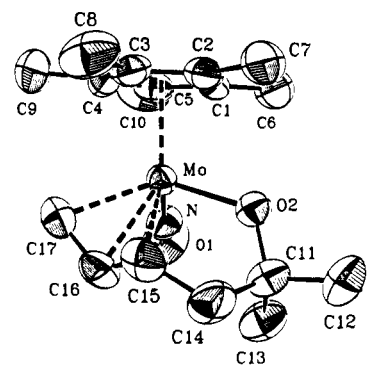

Figure 1. View of the solid-state molecular structure of Cp*Mo(NO)(η^4-*endo*-$CH_2CHCHCH_2CMe_2O$) (2) (50% thermal ellipsoids; H atoms omitted for clarity).

Results and Discussion

Reactions of Cp'Mo(NO)(η^4-*trans*-diene) Complexes with Acetone. A. CpMo(NO)(η^4-*trans*-butadiene). When CpMo(NO)(η^4-*trans*-butadiene) is treated with acetone according to method A described in the Experimental Section, a ligand-coupling reaction occurs (eq 1).

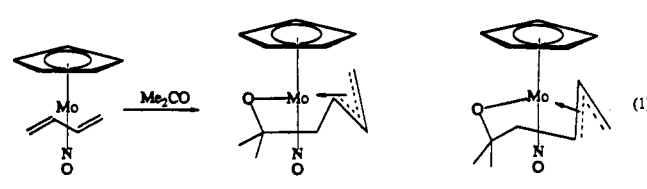

(1)

1A: *endo* 1B: *exo*

As shown, two products, one in which the allyl portion of the coupled ligand is endo (**1A**) and one in which the allyl is exo (**1B**) with respect to the Cp ligand, result from conversion 1 in approximately equal amounts. These two complexes, **1A** and **1B**, are initially identifiable by their different ν_{NO}'s (1632 and 1616 cm^{-1}, respectively) in an Et_2O extract of the final reaction mixture once the acetone

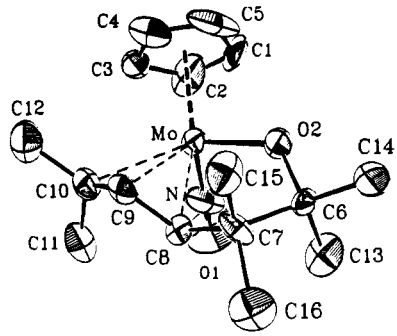

Figure 2. View of the solid-state molecular structure of CpMo(NO)[η^4-*exo*-C(Me)$_2$CHCHC(Me)$_2$C(Me)$_2$O] (**3B**). This is one of the two independent (and essentially identical) molecules in the asymmetric unit. (A view of the second molecule is presented in the supplementary material.)

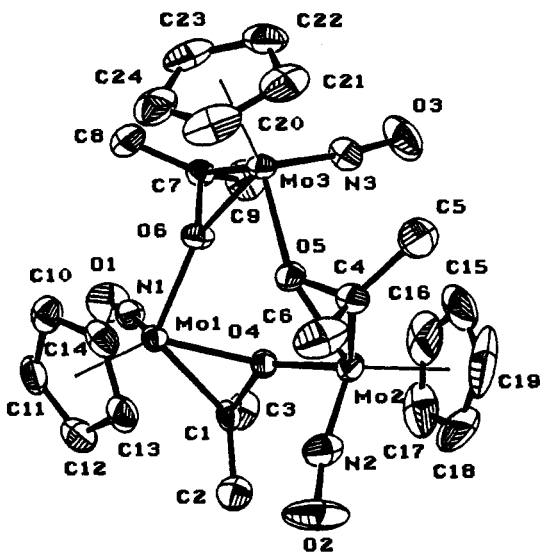

Figure 3. View of the solid-state molecular structure of [CpMo(NO)]$_3$(μ_2-η^2-η^1-OCMe$_2$)$_3$·THF (**4**).

has been removed under reduced pressure. Then, the two complexes may be separated by chromatography on Florisil. If Et_2O is used as eluant, the *exo*-allyl complex (**1B**) may be isolated; if Et_2O/THF (1:1) is employed, the *endo*-allyl complex (**1A**) is obtained. The physical and analytical data for these and the other monomeric complexes characterized during these studies are contained in Tables I–IV.

The complexes **1A** and **1B** are yellow, microcrystalline solids that dissolve in common organic solvents to give bright yellow solutions. They are moderately air-stable as solids and may be handled in air for short periods of time with no noticeable decomposition occurring. In solutions, however, they are much more air-sensitive and decompose to give colorless solutions with sludgy, brown precipitates. The IR spectra of **1A** and **1B** in Et_2O exhibit ν_{NO}'s at 1632 and 1616 cm^{-1}, respectively, indicative of their possessing terminal, linear nitrosyl ligands. The fact that the ν_{NO} of **1A** is of higher energy than that exhibited by **1B** indicates that there is more electron density available at the metal center for back-bonding to the NO ligand in **1B** than in **1A**. This presumably reflects the difference in bonding of the allyl portion of the coupled ligand to the metal center.

NMR Spectral Studies of 1A and 1B. The complexes **1A** and **1B** exhibit comparable NMR spectral properties (Tables II–IV). Due to the complex coupling network extant in these systems, J_{HH} for most of the multiplets in their ^{1}H NMR spectra may not be measured directly from

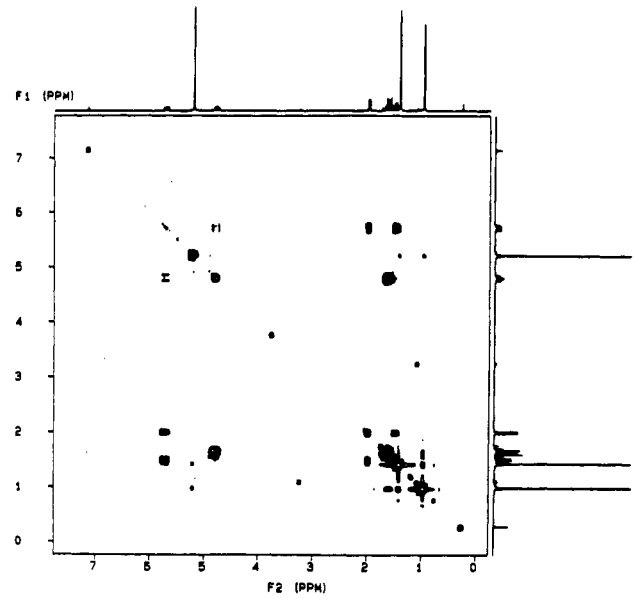

Figure 4. 300-MHz 2D-COSY NMR spectrum of **1A**.

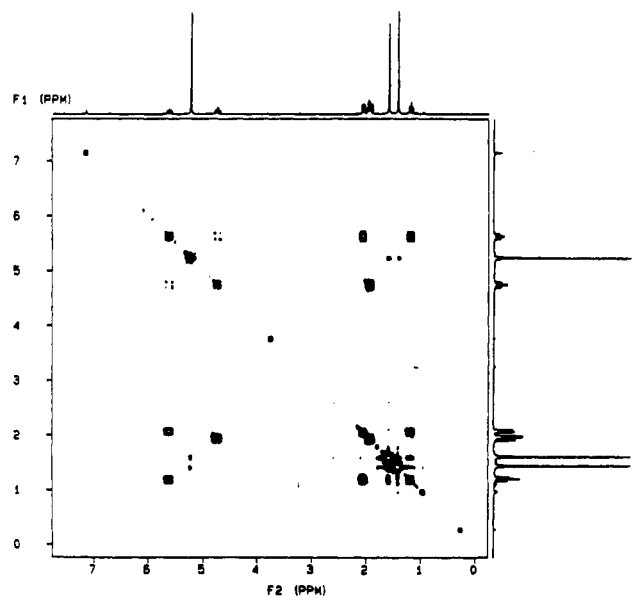

Figure 5. 300-MHz 2D-COSY NMR spectrum of **1B**.

these spectra. Indeed, the assignment of which protons are coupled with one another is most easily accomplished with a 2D-COSY NMR experiment, the 2D-COSY NMR spectra of **1A** and **1B** being shown in Figures 4 and 5, respectively. These latter spectra allow immediate assignment of the coupling networks and illustrate the complex nature of the coupling exhibited by these compounds. The final assignments of the ^{1}H NMR spectra of **1A** and **1B** are listed in Table II.

The ^{13}C NMR spectra of **1A** and **1B** are also very similar qualitatively. Assignments of the resonances to the specific carbons of **1A** and **1B** are contained in Table III. The most remarkable feature of these spectral data is the $^1J_{CH}$ measured from the gated decoupled ^{13}C NMR spectra. Specifically, the triplets in the spectra, due to C_1 and C_4 (Tables III and IV), indicate that one of the carbons is sp^2-hybridized ($^1J_{CH}$ for **1A** 41.4 ppm, 155.2 Hz; $^1J_{CH}$ for **1B** 42.2 ppm, 153.7 Hz) while the other is sp^3-hybridized ($^1J_{CH}$ for **1A** 48.9 ppm, 129.0 Hz; $^1J_{CH}$ for **1B** 46.9 ppm, 127.5 Hz). This is the first clear indication that the ligands have coupled. If the products of the reaction were complexes in which the two ligands had not coupled, all the

Table VII. Final Positional (Fractional × 10^4, Mo × 10^5) and Equivalent Isotropic Thermal Parameters (10^3U, Å^2) for CpMo(NO)[η^4-*exo*-C(Me)$_2$CHCHC(Me)$_2$C(Me)$_2$O] (3B)

atom	x	y	z	U_{eq}
Mo	4001 (16)	505 (12)	-20258 (12)	31
O1	1024 (17)	-2161 (11)	-2790 (13)	101
O2	-1576 (12)	-38 (9)	-1683 (8)	43
N	649 (17)	-1289 (13)	-2563 (11)	60
C1	1549 (34)	833 (21)	-203 (17)	83
C2	2574 (28)	543 (20)	-703 (19)	79
C3	2761 (23)	1199 (18)	-1153 (15)	61
C4	1847 (25)	1885 (14)	-885 (14)	48
C5	1012 (22)	1713 (21)	-317 (19)	85
C6	-2956 (17)	-716 (12)	-2442 (13)	33
C7	-3016 (19)	-426 (14)	-3415 (12)	38
C8	-1581 (19)	-558 (12)	-3669 (12)	28
C9	-458 (19)	229 (13)	-3511 (12)	34
C10	1002 (20)	117 (14)	-3524 (13)	43
C11	1289 (19)	-1002 (16)	-4285 (14)	57
C12	2065 (20)	1064 (16)	-3401 (15)	61
C13	-2983 (20)	-1904 (14)	-2811 (15)	59
C14	-4201 (20)	-391 (15)	-1896 (14)	57
C15	-3277 (18)	703 (14)	-3026 (14)	51
C16	-4325 (20)	-1276 (15)	-4394 (15)	59
Mo′	22484 (18)	-44025 (12)	-16684 (13)	39
O1′	3396 (15)	-6261 (10)	-1628 (12)	80
O2′	388 (13)	-4390 (9)	-1178 (9)	46
N′	2777 (16)	-5590 (11)	-1731 (12)	56
C1′	3304 (32)	-3020 (22)	129 (14)	99
C2′	4440 (27)	-3445 (16)	-314 (17)	71
C3′	4556 (20)	-3185 (15)	-1103 (16)	51
C4′	3528 (23)	-2537 (14)	-1106 (19)	66
C5′	2758 (26)	-2515 (17)	-417 (21)	71
C6′	-927 (21)	-5227 (15)	-1739 (16)	60
C7′	-1296 (19)	-5412 (14)	-2928 (14)	39
C8′	120 (22)	-5561 (14)	-3268 (13)	46
C9′	1108 (23)	-4877 (14)	-3403 (15)	51
C10′	2576 (21)	-4918 (14)	-3385 (14)	50
C11′	3018 (24)	-5993 (17)	-3870 (16)	73
C12′	3442 (26)	-4109 (17)	-3629 (15)	83
C13′	-751 (20)	-6290 (15)	-1747 (15)	62
C14′	-2152 (21)	-4827 (15)	-1196 (16)	64
C15′	-1784 (23)	-4422 (15)	-2950 (18)	82
C16′	-2531 (20)	-6472 (14)	-3765 (13)	56

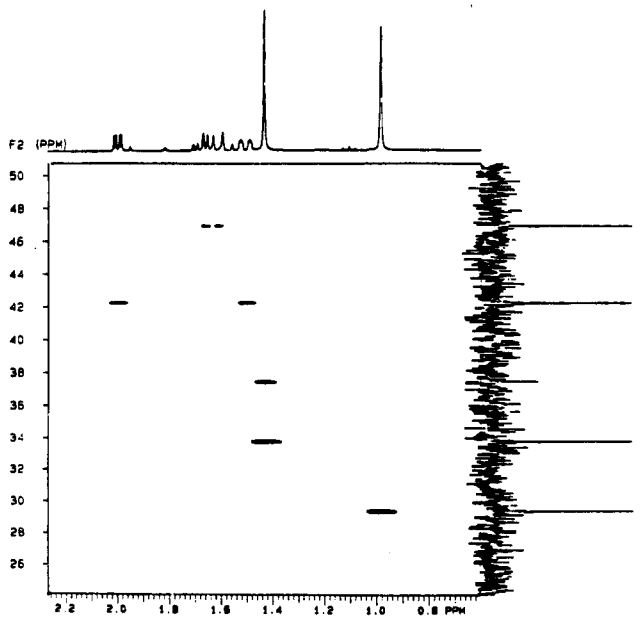

Figure 6. Partial 2D-HETCOR NMR spectrum of **1A** in C_6D_6.

carbons of the diene ligand would still be sp^2-hybridized as they are in the starting diene complex.[5] The remainder of the ^{13}C NMR spectra are as expected, each exhibiting two quartets assignable to the methyl carbons of the acetone fragment, a doublet of pentets due to the cyclo-

Table VIII. Final Positional (Fractional × 10^4, Mo × 10^5, THF × 10^3) and Equivalent Isotropic Thermal Parameters (10^3U, Å^2) for [CpMo(NO)]$_3$(μ_2-η^2-η^1-OC(Me$_2$)$_3$•THF (4)

atom	x	y	z	$U_{iso/eq}$
Mo1	43260 (5)	26166 (7)	14545 (4)	24
Mo2	22893 (6)	16791 (7)	949 (5)	30
Mo3	22577 (5)	48887 (7)	9001 (4)	25
O1	4735 (6)	2347 (8)	3001 (4)	58
O2	3442 (7)	686 (8)	-901 (4)	76
O3	436 (5)	3992 (8)	1132 (5)	65
O4	3199 (4)	1578 (5)	1050 (3)	29
O5	2525 (4)	3575 (5)	154 (3)	30
O6	3294 (4)	3908 (6)	1448 (3)	30
N1	4509 (5)	2455 (7)	2368 (4)	33
N2	3037 (6)	1167 (8)	-466 (4)	42
N3	1208 (6)	4279 (7)	1051 (4)	34
C1	3889 (6)	671 (8)	1313 (5)	30
C2	4229 (7)	-94 (9)	787 (6)	42
C3	3687 (8)	87 (10)	1946 (5)	44
C4	2021 (7)	3320 (9)	-510 (5)	37
C5	1072 (8)	3853 (11)	-674 (6)	54
C6	2595 (10)	3541 (11)	-1082 (7)	62
C7	2914 (6)	4510 (8)	1966 (4)	27
C8	3584 (8)	5336 (10)	2404 (6)	52
C9	2387 (9)	3696 (11)	2380 (6)	51
C10	5369 (7)	4094 (10)	1228 (5)	38
C11	5874 (7)	3052 (10)	1461 (6)	43
C12	5659 (7)	2132 (10)	960 (6)	42
C13	5026 (7)	2626 (10)	394 (5)	39
C14	4862 (6)	3812 (9)	567 (5)	35
C15	705 (10)	1498 (14)	257 (14)	89
C16	1181 (11)	821 (18)	733 (9)	80
C17	1623 (10)	-75 (13)	450 (11)	76
C18	1387 (12)	23 (15)	-2656 (12)	89
C19	811 (12)	1048 (19)	-376 (10)	101
C20	2677 (10)	6438 (10)	130 (6)	52
C21	1718 (9)	6486 (9)	154 (6)	51
C22	1635 (8)	6814 (10)	845 (7)	49
C23	2524 (10)	6920 (9)	1223 (6)	53
C24	3152 (9)	6693 (10)	775 (7)	53
O7 (0.5)[a]	326 (18)	777 (3)	2123 (12)	119 (8)
O8 (0.5)	130 (3)	869 (4)	273 (2)	118 (12)
C25 (0.5)	84 (4)	869 (4)	232 (3)	128 (15)
C26 (0.5)	143 (4)	798 (6)	311 (3)	152 (19)
C27 (0.5)	142 (3)	713 (5)	310 (2)	122 (14)
C28 (0.5)	57 (4)	672 (5)	260 (3)	172 (24)
C29 (0.5)	31 (5)	857 (7)	236 (4)	140 (26)
C30 (0.5)	10 (4)	705 (5)	252 (3)	91 (15)
C31 (0.5)	88 (4)	679 (5)	302 (3)	90 (141)
C32 (0.5)	181 (4)	804 (6)	285 (3)	106 (17)

[a] Atoms O7–C32 are those of the disordered tetrahydrofuran.

pentadienyl carbons, two doublets assignable to carbons 2 and 3 of the diene fragment, and a singlet due to the O-bound carbon of the acetone fragment. The ^{13}C chemical shifts of the resonances of the two isomers are different, indicative of slight differences in the chemical environments of the carbons. Most notable is the chemical shift of carbon 2 of the coupled ligand. In **1A** this carbon resonates at 131.1 ppm, while in **1B** the resonance occurs at 117.0 ppm. Carbon 2 in **1A**, the *exo*-allyl complex, is nearer to the cyclopentadienyl ligand than carbon 2 in the *endo*-allyl compound, and this may be the cause of the different environments exhibited by these two carbons. Another possible cause for the difference between the chemical shifts of these two resonances is a difference in the bonding in which those carbons are involved. If the two allyl moieties are asymmetrically bonded to the metal, it is likely that the asymmetry is different in **1A** than it is in **1B**.

Final assignment of the ^{1}H and ^{13}C NMR spectra of these two compounds is made possible by a 2D-HETCOR NMR experiment. In this fashion, the proton resonances are cross assigned to the carbon resonances. The partial

Table IX. Selected Bond Lengths (Å) and Bond Angles (deg) for Complexes 2, 3B, and 4[a]

	2	3B[b]	4[c]
Mo–O	2.029 (4)	2.01 (1)	2.08 (1)
			2.11 (1)
Mo–N	1.766 (5)	1.75 (2)	1.75 (1)
Mo–CP[d]	2.053 (3)	2.05 (1)	2.05 (1)
Mo–allyl[e]	2.409 (6)	2.46 (2)	
	2.305 (6)	2.29 (2)	
	2.245 (8)	2.37 (2)	
Mo–C(O)Me_2			2.17 (1)
N–O	1.208 (6)	1.22 (2)	1.22 (1)
C–O	1.418 (7)	1.42 (2)	1.40 (1)
C–C chain[f]	1.540 (10)	1.62 (2)	
	1.493 (11)	1.49 (2)	
	1.330 (11)	1.36 (2)	
	1.422 (11)	1.39 (2)	
Mo–N–O	170.9 (6)	168 (1)	172 (1)
Mo–O–C	122.6 (4)	125 (1)	74 (1)
Mo–C–O			67 (1)
Me–C–Me			113 (1)

[a] Full listing in the supplementary material. [b] For **3B**, mean values of the two molecules in the asymmetric unit are listed. [c] For **4**, mean values of the three Mo centers are listed. [d] CP = centroid of the cyclopentadienyl ring. [e] Mo–C15–17 in **2**; Mo–C8–10 in **3B**. [f] C11···C17 in **2**; C6···C10 in **3B**.

2D-HETCOR NMR spectrum of **1A** is shown in Figure 6, the spectrum encompassing ca. 0.6–2.2 ppm in the proton range and ca. 24–50 ppm in the carbon range. From these experiments it is clear that the complete structural assignment of these complexes is possible by using NMR spectroscopy alone.

B. Cp*Mo(NO)(η^4-*trans*-butadiene). Treatment of Cp*Mo(NO)(η^4-*trans*-butadiene)with acetone proceeds in a manner similar to that for its Cp analogue. However, the reaction takes longer to go to completion (12 h). A workup procedure similar to that presented above for the Cp complex results in the isolation of a single product, namely Cp*Mo(NO)(η^4-$CH_2CHCHCH_2CMe_2O$) (**2**), in which the allyl portion is coordinated in an endo fashion to the molybdenum. This complex may be characterized in the same manner as that described above for the Cp analogue, and the characterization data are included in Tables I–IV.

Single crystals of compound **2** were obtained from a concentrated hexanes solution of the complex, and one of the crystals was used for an X-ray crystallographic analysis. The final ORTEP plot obtained is shown in Figure 1, and selected bond lengths and angles are listed in Table IX. Notable structural features exhibited by this complex are those that describe the allyl portion of the coupled ligand. First, the allyl is oriented endo with respect to the cyclopentadienyl ligand. The three carbons of the allyl fragment (C15–C17 in Figure 1) are somewhat asymmetrically bonded to the molybdenum center. This is clearly evident since the C15–C16 bond (1.330 (11) Å), in the range of a carbon–carbon double bond, is slightly shorter than the C16–C17 bond (1.422 (11) Å), whose bond length is intermediate between a C–C single and a double bond. Similar asymmetric bonding of a π-allyl ligand to the CpM(NO) fragment has been noted in other systems.[16] As expected, the C–C bond of the allyl fragment in **2**, which has more double-bond character (i.e. C15–C16), is situated trans to the NO group, a good π-acceptor ligand.

The molybdenum–carbon distances are also illustrative of the asymmetrical bonding of the allyl fragment of the coupled ligand in **2**. Thus, the Mo–C17 bond length (2.245 (7) Å) is within the range expected for a Mo–C single bond[17] and, indeed, very close to the length of the Mo–C σ-bond determined for related complexes.[1] The Mo–C16 (2.305 (6) Å) and Mo–C15 (2.409 (6) Å) bonds are significantly longer than the Mo–C17 bond, and this also is consistent with the asymmetric bonding invoked for the allyl portion of the ligand, i.e.

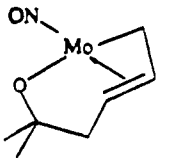

Mo = CpMo

This observation contrasts to the asymmetric allyl bonding extant in the molecular structure of CpMo(NO)[η^4-C-$(Me)_2CHCHC(Me)_2C(Me)C(Ph)$],[1] where the Mo–allyl–carbon bond lengths are greater than 2.3 Å and the carbon–carbon bond distances in the allyl fragment are not indicative of any asymmetry.

That the Mo–allyl linkage is tending toward asymmetry in **2** is also evident in its ^{13}C NMR spectrum (see Tables III and IV). Thus, the chemical shift of the signal attributable to C17 (C_1 in Table III) is 47.7 ppm, which is in the chemical-shift range usually associated with sp^3-hybridized carbon atoms in transition-metal–alkyl complexes, whereas C16 (C_2 in Table III) resonates at 118.8 ppm in the region expected for sp^2-hybridized carbons bound to transition metals.[18] The $^1J_{CH}$ associated with C17 (150.5 Hz), however, indicates some sp^2 character for this carbon in solutions of the complex, an observation which in turn implies that some molecular fluxionality probably occurs in solution.

Other structural features to note about **2** are the essentially linear Mo–NO linkage (170.9 (6)°) and the Mo–N (1.766 (5) Å) and N–O (1.208 (6) Å) distances, which are in the same range as those seen for CpMo(NO)[η^4-C-$(Me)_2CHCHC(Me)_2C(Me)C(Ph)$][1] and are indicative of a normal Mo–NO linkage.

C. CpMo(NO)(η^4-*trans*-2,5-dimethyl-2,4-hexadiene). Method A. The reaction between CpMo(NO)(η^4-*trans*-2,5-dimethyl-2,4-hexadiene) and acetone is fairly rapid, being complete in 1–3 h under ambient conditions. The products of the reaction are the *endo*-allyl (**3A**) and *exo*-

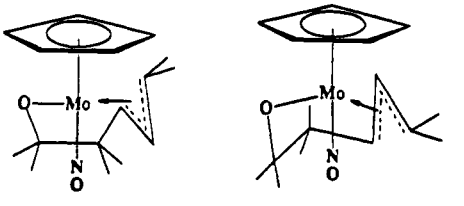

3A: *endo* **3B**: *exo*

allyl (**3B**) complexes, which are initially present in varying ratios (**A:B** ≈ 3:1–4:1) depending on the reaction time. The complexes exhibit different ν_{NO}'s in IR spectra of their solutions (e.g. **3A**, 1634 cm^{-1} and **3B**, 1616 cm^{-1} in hexanes). Interestingly, the endo isomer converts quickly (<3 h at 20 °C) to the *exo*-allyl isomer. The ^1H NMR spectra of **3A** and **3B** in C_6D_6 are shown in Figure 7. A notable

(16) (a) Greenhough, T. J.; Legzdins, P.; Martin, D. T.; Trotter, J. *Inorg. Chem.* **1979**, *11*, 3268. (b) Faller, J. W.; Shvo, Y. *J. Am. Chem. Soc.* **1980**, *102*, 5396.

(17) Orpen, A. G.; Brammer, L.; Allen, F. H.; Kennard, O.; Watson, D. G.; Taylor, R. *J. Chem. Soc., Dalton Trans.* **1989**, S1.

(18) Faller, J. W.; Chen, C. C.; Mattina, M. J.; Jakubowski, A. *J. Organomet. Chem.* **1973**, *52*, 361.

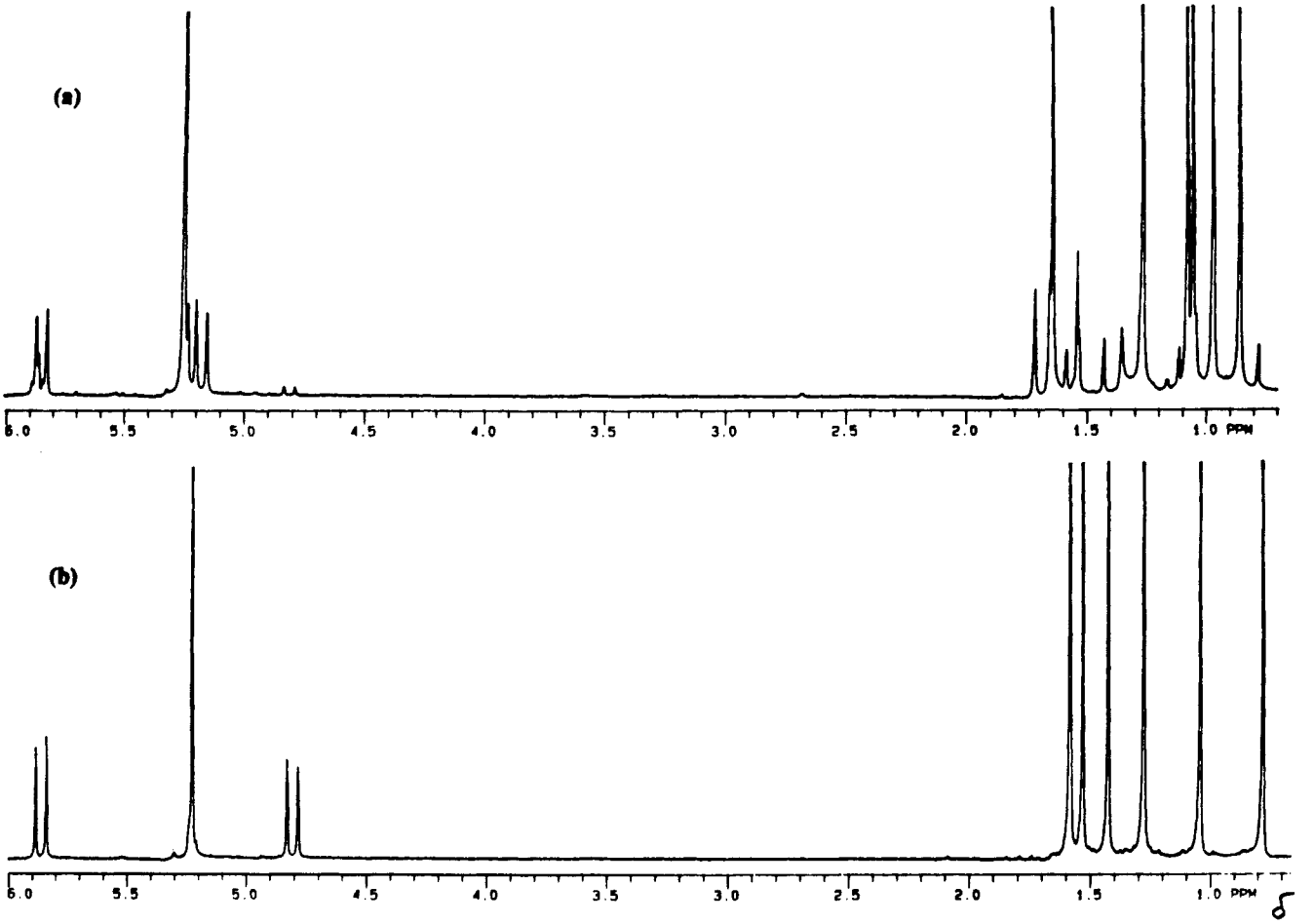

Figure 7. 300-MHz ^{1}H NMR spectra of (a) **3A** and (b) **3B** in C_6D_6.

feature of these spectra involves the resonances assignable to **3B** in the spectrum of **3A** even though the spectrum was obtained immediately after preparation of the NMR sample from pure **3A**. The rapid and irreversible isomerization of the *endo*-allyl complex to its exo isomer is presumably due to the strong steric interactions between the methyl groups of the diene fragment and the cyclopentadienyl ligand. The source of these interactions is evident in molecular models of **3A** and **3B**, which clearly illustrate the relief of steric strain that occurs upon isomerization to the *exo*-allyl isomer. This explanation may also account for the fact that this isomerization is not observed in the system where the diene ligand does not bear methyl substituents (i.e. **1A** and **1B**).

The ^{13}C NMR spectral data for **3B** are collected in Tables III and IV. Notable in these data is the high chemical shift of the resonance due to carbon 2 at 129.3 ppm, indicative of the presence of an *exo*-allyl ligand. The presence of the four methyl substituents on the diene ligand (as compared to **1A** and **1B** above) precludes complete assignment of each of the signals of the spectra to individual carbon atoms in the structure. For example, C_1 and C_4 of the coupled ligand exhibit singlets in the gated-decoupled ^{13}C NMR spectrum and are assignable to the signals at 71.8 and 46.2 ppm, respectively. The hybridization of those carbons is not, however, determinable from the ^{13}C NMR signals. In other words, the physical and analytical data do not show conclusively that the diene and the acetone ligands have coupled.

An X-ray crystallographic analysis of **3B** was therefore undertaken on a crystal grown from a saturated hexanes solution of the complex. The crystal structure of **3B** contains two independent molecules in the asymmetric unit. The ORTEP plot of the solid-state molecular structure of one of these molecules is shown in Figure 2, and selected bond lengths and angles are listed in Table IX. As illustrated in Figure 2, the two ligands have indeed coupled to form a σ,π-*exo*-allyl complex. The intramolecular parameters of the allyl fragment and the molybdenum–allyl-carbon distances in **3B** are not indicative of any asymmetry in the molybdenum–allyl bonding and are consistent with the results obtained from the ^{13}C NMR experiments (Table III). This symmetric attachment of the allyl fragment to the metal center in **3B** thus contrast to that observed for **2** (vide supra). The molybdenum–nitrosyl linkage is almost linear (mean 168 (1) °) and the Mo–N (1.75 (2) Å) and N–O (1.22 (2) Å) bond distances are consistent with the existence of a normal, terminal nitrosyl ligand. The molybdenum–oxygen bond distance of 2.01 (1) Å is similar to that seen in the molecular structure of **2** and is in the range expected for a Mo–O σ-bond.[17,19] The O–C bond distances in both **2** (O2–C11 = 1.418 (7) Å) and **3B** (O2–C6 = 1.42 (2) Å) are in the range expected for a C–O single bond.[20]

The reactivity of these molybdenum η^4-*trans*-diene complexes toward acetone may be compared to that exhibited by other diene complexes such as those involving group 4 and 5 metals.[21] In this regard, zirconium systems

(19) Jacobson, S. E.; Tang, R.; Mares, R. *Inorg. Chem.* **1978**, *17*, 3055.
(20) Allen, F. H.; Kennard, O.; Watson, D. G.; Brammer, L.; Orpen, A. G.; Taylor, R. *J. Chem. Soc., Perkin Trans.* **1987**, S1.
(21) Yasuda, H.; Okamoto, T.; Mashima, K.; Nakamura, A. *J. Organomet. Chem.* **1989**, *363*, 61 and references cited therein.

of the type $Cp_2Zr(\eta^4$-diene) have been particularly extensively studied. For these latter complexes, experimental conditions may be controlled such that the nature of the reacting species (i.e. η^4-*cis*-diene or η^4-*trans*-diene) is known. In its reaction with ketones, $Cp_2Zr(\eta^4$-*trans*-isoprene) yields different products depending on the reaction conditions.[22] These insertion products vary in stereochemistry and regiochemistry, i.e.

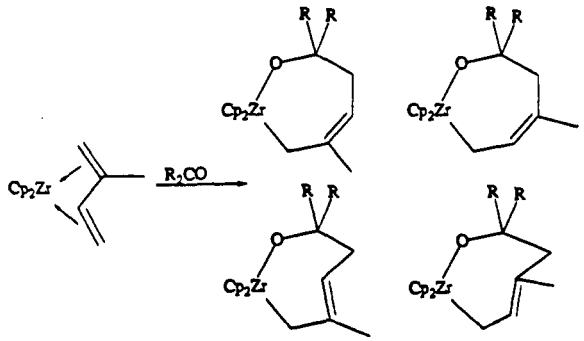

Thus, the thermal reaction of $Cp_2Zr(\eta^4$-*trans*-isoprene) yields both the *Z* and *E* isomers with preferential insertion occurring at the sterically most crowded position, whereas the photochemical reaction effects insertion at the sterically least crowded position.[23] These reactions are believed to proceed via an η^2-diene zirconium complex that first coordinates a ketone ligand and then couples the ligands to afford the 16-valence-electron product complex, i.e.

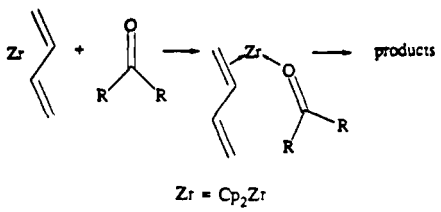

Zr = Cp_2Zr

R_2CO = benzophenone, acetone, cyclodecanone, acetophenone, pinacolone, isobutyraldehyde

Furthermore, certain $Cp_2Zr(\eta^4$-*trans*-diene) complexes incorporate 2 equiv of the ketone under mild conditions to afford 1,3-dioxazirconacyclo-6-nonene derivatives quantitatively.[21]

In comparison with these zirconocene systems, the reactions involving mediation by the molybdenum nitrosyl complexes are cleaner. Thus, the products of the reactions of the CpMo(NO)(η^4-*trans*-diene) complexes with acetone are solely the σ,η^3-allyl complexes. The frontier orbitals of the CpMo(NO) fragment are believed to be pointing away from the cyclopentadienyl ring down the "legs of the piano stool" opposite the nitrosyl ligand,[4] and in each case of ligand coupling, the position of the allyl fragment is consistent with this. The positions of the frontier orbitals on the two fragments, Cp_2Zr and CpMo(NO), thus apparently determine the mode of coordination of the coupled ligand. This effect may be significant in determining the subsequent chemistry of these complexes and the stereochemistry of any organic products obtained when the ligand is removed from the metal center.

These studies of the coupling of organic molecules in the presence of the Cp'Mo(NO) fragment have thus far been fruitful. Preliminary studies indicate that these molybdenum diene complexes also react very quickly with acetonitrile to form at least two products (by IR spectroscopy). Future studies will explore the coupling of butadienes with other unsaturated organic molecules. Studies are also currently in progress to remove the coupled ligands from the molybdenum and to determine the nature of the organic products of these latter reactions.

Method B. If the reaction of CpMo(NO)(η^4-*trans*-2,5-dimethyl-2,4-hexadiene) with acetone is allowed to continue for extended periods of time (>5 h), the *endo*-allyl complex, **3A**, is isolated in significantly reduced yields. Indeed, if the reaction is left for 15 h at ambient conditions, then there is no **3A** detectable in the final reaction mixture. The only organometallic product that may be isolated from the hexanes extraction of the reaction mixture is **3B**. There is also a significant amount of a hexanes-insoluble product produced. This brown precipitate dissolves in THF to give a pale yellow solution whose IR spectrum exhibits a single nitrosyl band at 1593 cm^{-1}. Concentration of this THF solution followed by cooling to −20 °C overnight allows isolation of the complex $[CpMo(NO)]_3(\mu_2$-η^2-η^1-$OCMe_2)_3$ (**4**) as a THF solvate. The elemental analysis data for this trimer are consistent with this formulation, but the parent ion is not observed in the low-resolution mass spectrum. Rather, there is a peak assignable to the trimer minus the [CpMoNO(Me_2CO)] fragment.

The trimer, **4**, is isolable as a bright yellow powder from THF. It is insoluble in hexanes and Et_2O, very soluble in CH_2Cl_2, and less so in THF. It is not air-sensitive as a solid, remaining unchanged (as monitored by ^1H NMR spectroscopy) after exposure to air for 72 h. A crystal suitable for X-ray structural analysis was obtained from a concentrated THF solution of **4**. The solid-state molecular structure established by this analysis is shown in Figure 3, and selected bond lengths and angles are presented in Table IX. The ORTEP plot in Figure 3 shows that the structure of **4** consists of three four-legged piano stool monomeric units connected by Mo–acetone–Mo linkages, i.e.

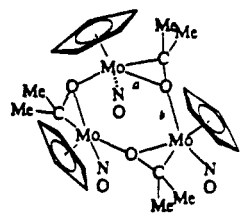

The nitrosyl ligands are all approximately linear (Mo–N–O (average) = 172 (1)°). The most notable structural features are those exhibited by the μ_2-η^2-η^1-acetone ligands. The angles around the O-bound carbon of the acetone group are quite distorted. The H_3C–*C*–CH_3 angles are approximately 113 (1)° (average), consistent with the existence of a tetrahedral sp^3-hybridized carbon. The average Mo–C–O angle, however, is 67 (1)°, indicating significant distortion of the hybridization of that carbon from the expected sp^3-hybridization and from the sp^2-hybridization of that carbon in free acetone. The angle about the oxygen (average Mo–O–C = 74 (1)°) is also indicative of distortion, as it deviates from the expected 120°.

The bond lengths within the Mo–η^2-acetone linkage are also noteworthy. The carbon–oxygen length of 1.40 (1) Å (average) is close to that expected for a carbon–oxygen single bond[20] and is not lengthened, as it is in strained-ring epoxides. It is also similar to that seen in the molecular structures of **2** and **3B** (Table IX). It is longer than those exhibited by $(PPh_3)_3Mo(\eta^2$-PhCHO) (1.33 Å)[24] or

(22) Yasuda, H.; Nakamura, A. *Angew. Chem., Int. Ed. Engl.* **1987**, *26*, 723 and references cited therein.

(23) (a) Kai, Y.; Kanehisa, N.; Miki, K.; Kasai, N.; Akita, M.; Yasuda, H.; Nakamura, A. *Bull. Chem. Soc. Jpn.* **1983**, *56*, 3735. (b) Erker, G.; Dorf, U. *Angew. Chem., Int. Ed. Engl.* **1983**, *22*, 777.

$Cp_2Mo(\eta^2\text{-}CH_2O)$ (1.36 Å),[25] both of which have partial carbon–oxygen double-bond character. Correspondingly, the Mo–C bond distance of 2.17 (1) Å (average) in **4** is shorter than those exhibited by the η^2-ketone ligands in the $Mo(\eta^2\text{-}PhCHO)$ (2.26 Å)[24] and $Mo(\eta^2\text{-}H_2CO)$ (2.25 Å)[25] complexes. These values are significantly smaller than that seen in the molecular structure of $CpMo(NO)[\eta^4\text{-}C(Me)_2CHCHC(Me)_2C(Me)C(Ph)]$, the alkyne-coupled product,[1] but still within the range of a single molybdenum–carbon σ-bond. The Mo–O bond distance (a in the drawing) of 2.08 (1) Å (average) is similar in magnitude to those of the other molybdenum η^2-ketone complexes, and indeed, the O–Mo distance (b, 2.11 (1) Å (average)) is in that same range.

The reaction that results in the formation of the trimeric complex (eq 2) is most remarkable. The fact that a trimer of molybdenum bridged by η^2-acetone ligands is formed

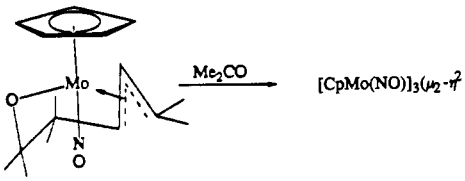

$$[CpMo(NO)]_3(\mu_2\text{-}\eta^2\text{-}\eta^1\text{-}OCMe_2)_3 \quad (2)$$

in the presence of excess acetone instead of a monomer with two acetone ligands bonded in an η^1-fashion, $CpMo(NO)(OCMe_2)_2$, is most surprising, given the ease with which other Lewis bases, L, form analogous 18-electron $CpMo(NO)L_2$ complexes.[26] It can only be surmised that due to the strength of the Mo–O single bonds, the trimer (however it is formed) is the thermodynamically most stable species, which, once formed, does not readily break up under the existing experimental conditions. The trimeric complex may be broken, however, with 1,3-(diphenylphosphino)propane (dppp) to form the dppp complex, analogues of which have been prepared previously.[26]

$$[CpMo(NO)]_3(\mu_2\text{-}\eta^2\text{-}\eta^1\text{-}OCMe_2)_3 + \text{dppp} \rightarrow CpMo(NO)(\text{dppp}) + \text{other products} \quad (3)$$

The exact mode of formation of $[CpMo(NO)]_3(\mu_2\text{-}\eta^2\text{-}\eta^1\text{-}OCMe_2)_3$ is currently not known. An interesting observation may be made, however. The *endo*-allyl complex, $CpMo(NO)(\sigma,\eta^3\text{-}CMe_2CHCHCMe_2CMeCPh)$,[1] formed from the reaction of $CpMo(NO)(\eta^4\text{-}trans\text{-}2,5\text{-}dimethyl\text{-}2,4\text{-}hexadiene)$ and 1-phenylpropyne, does not react with acetone, even after being stirred in neat acetone for more than 2 weeks. However, **3B** is converted to **4** upon being stirred in acetone/THF at room temperature for 3 days. Thus, at present, we believe that the trimeric complex is most likely formed from the reaction of the *exo*-allyl complex with acetone. So far, no evidence for the formation of an analogous trimeric complex in the butadiene systems (**1** or **2**) exists. For this reason, we believe that the steric repulsions extant in the tetramethyl-substituted diene system contribute to the thermodynamic driving force of this reaction and cause the diene ligand to somehow dissociate from the metal center. We have not as yet ascertained the nature of the organic byproducts of the reaction. We are presently designing the methodology for the isolation and identification of these species. It will be especially interesting to see if the organic byproducts of the reaction have incorporated more than one molecule of acetone.

In closing, it may be noted that the related 14-valence-electron Cp_2Zr fragment forms a trimeric complex quite similar to **4**, namely tris[(η^2-formaldehyde)-zirconocene], which has also been structurally characterized.[27] While the latter complex is not synthesized by a reaction analogous to that portrayed in eq 2, but rather by prolonged carbonylation of $[Cp_2ZrH_2]_x$, its existence nevertheless indicates that both the CpMo(NO) and Cp_2Zr fragments possess a propensity to attach ketones in a bridging[28] rather than a terminal fashion so that the metal centers may attain the favored 18-valence-electron configuration. An explanation of this property awaits a detailed theoretical analysis of the bonding in these remarkable species.

Acknowledgment. We are grateful to the Natural Sciences and Engineering Research Council of Canada for support of this work in the form of grants to P.L. and J.T. P.L. also acknowledges fruitful conversations with members of the Inorganic and Structural Chemistry Group (INC-4) at Los Alamos National Laboratory.

Registry No. **1A**, 136806-08-1; **1B**, 136890-01-2; **2**, 136806-06-9; **3A**, 136890-00-1; **3B**, 136806-05-8; **4**, 136892-74-5; dppp, 6737-42-4; $CpMo(NO)(\eta^4\text{-}trans\text{-}2,5\text{-}dimethyl\text{-}2,4\text{-}hexadiene)$, 95123-27-6; $Cp'Mo(NO)(\eta^4\text{-}trans\text{-}butadiene)$, 136806-07-0; CpMo(NO)(dppp), 136806-09-2.

Supplementary Material Available: Tables of anisotropic thermal parameters for the non-hydrogen atoms, positional and thermal parameters for the hydrogen atoms, and bond lengths and bond angles for each of the complexes **2**, **3B**, and **4** and a view of the second molecule of **3B** (14 pages); listings of the observed and calculated structure factors for all three complexes (100 pages). Ordering information is given on any current masthead page.

(24) Clark, G. R.; Headfold, C. E. L.; Marsden, K.; Roper, W. R. *J. Organomet. Chem.* **1982**, *231*, 335.
(25) Gambarotta, S.; Floriani, C.; Chiesi-Villa, A.; Guastini, C. *J. Am. Chem. Soc.* **1985**, *107*, 2985.
(26) Hunter, A. D.; Legzdins, P. *Organometallics* **1986**, *5*, 1001.
(27) Kropp, K.; Skibbe, V.; Erker, G.; Krüger, C. *J. Am. Chem. Soc.* **1983**, *105*, 3353.
(28) For examples of other bridged ketone complexes, see: (a) Martin, B. D.; Matchett, S. A.; Norton, J. R.; Anderson, O. P. *J. Am. Chem. Soc.* **1985**, *107*, 7952. (b) Stella, S.; Floriani, C. *J. Chem. Soc., Chem. Commun.* **1986**, 1053. (c) Erker, G.; Dorf, U.; Czisch, P.; Petersen, J. L. *Organometallics* **1986**, *5*, 668. (d) Flores, J. C.; Mena, M.; Royo, P.; Serrano, R. *J. Chem. Soc., Chem. Commun.* **1989**, 617.